Supplementary Information

Figure S1. Fraction of input DNA with H3K4me3 modification measured by qPCR vs. normalized reads per million from ChIP-seq. Four hotspots were chosen across a range of H3K4me3 levels encompassing > 95% of all hotspots. Aliquots of the same DNA samples prior to library preparation for ChIP-seq were used for quantitative PCR. Filled and open symbols represent data from the two biological replicates used for sequencing (square – hotspot chr1 54.93 Mb, triangle – hotspot chr2 7.55 Mb, circle – hotspot chr2 14.79 Mb, diamond – hotspot chr1 170.45 Mb).

Figure S2. Hotspot central NDRs are longer than the immediate flanking linker DNA regions. *(A)* Schematic of an idealized PRDM9-modified hotspot showing nucleosome positions including the NDR and left and right linker DNA regions. *(B)* Distribution of $PRDM9^{Dom2}$ NDRs and flanking linker regions for hotspots with four nucleosomes (n = 2,842). *(C)* Distribution of $PRDM9^{Cst}$ NDRs and flanking linker regions for hotspots with four nucleosomes (n = 8,771).

Figure S3. Nucleosome organization at CTCF sites in spermatocytes. *(A) de novo* motif identified at CTCF peaks overlapping with H3K4me3 peaks identified in this study (n = 3,564). CTCF ChIP-seq positions provided by the mouse ENCODE Project collected from adult testis. *(B)* Aggregation plot of H3K4me3 modified nucleosomes from B6 mice at CTCF sites. Hypothetical positions of nucleosomes are shown above the plot with the mean NDR length in base pairs indicated. The central NDR identified for CTCF in this study is on average 134 bp (± 25). *(C)* Aggregation plot of nucleosome positions from MNase-seq of spermatocytes from B6 mice for the same positions as in B. *(D)* Similar to **C** except using MNase-seq data from B6-$Prdm9^{CAST\text{-}KI}$ mice. Nucleosome organization at CTCF sites is independent of *Prdm9* allele.

Figure S4. PRDM9^{Cst} binds hotspots in the NDR at the predicted PRDM9^{Cst} motif. *(A)* Mapping PRDM9^{Cst} binding at hotspot chr1 176.46 Mb. A representative EMSA shows specific binding only to PRDM9^{Cst}. Only oligo 2, which contains the consensus motif, can compete with the full-length labeled NDR for binding (lane 5). All lanes contained labeled DNA; otherwise the composition of the binding reactions is shown above the blot (B – PRDM9^{Dom2}, C – PRDM9^{Cst}). *(B)* H3K4me3 ChIP-seq coverage profile showing the position of nucleosomes, central NDR, and DNA positions used for EMSA (red bars indicate DNA that can bind PRDM9^{Cst}, black bars indicate nonbinding DNA, yellow bars show the position of the PRDM9^{Cst} motif). *(C)* The DNA sequence of oligo 2 indicating position base pairs that match the PRDM9^{Cst} consensus motif in Fig. 2F. *(D)* Comparison of the PRDM9^{Cst} motif inferred by ChIP-seq to previously identified PRDM9^{Cst} binding sites (Billings et al. 2013). The minimum hotspot DNA sequences that PRDM9^{Cst} binds to are shown. The individual base pairs that match the motif are formatted similar to the logo plot to highlight similarities at each position. Hotspot names and chromosome position to the nearest megabase are indicated to the right of the DNA sequence. For Esrrg1 the best match to the motif was found on the Crick strand, the opposite direction to how the binding site previously shown to align with PRDM9^{Cst}.

Figure S5. PRDM9^{Dom2} binds in the NDR at the predicted PRDM9^{Dom2}motif. *(A)* Mapping PRDM9^{Dom2} binding at hotspot chr11 89.47 Mb. A representative EMSA shows specific binding of this hotspot to PRDM9^{Dom2}. Only the unlabeled oligo 2, containing the consensus motif, can compete for binding the full-length labeled NDR (lanes 3 and 5). All lanes contained labeled DNA; otherwise the composition of the binding reactions is shown above the blot (B – PRDM9^{Dom2}, C – PRDM9^{Cst}). *(B)* H3K4me3 ChIP-seq coverage profile showing the position of nucleosomes, central NDR, and DNA positions used for EMSA (red bars indicate DNA that can bind PRDM9^{Dom2}; black bars indicate nonbinding DNA, yellow bars indicate the position of the

PRDM9^{Dom2} motif). *(C)* The DNA sequence of oligo 2 indicating base pairs that match the PRDM9^{Dom2} consensus motif in Fig. 2E.

Figure S6. Meiotic crossing over is restricted to regions of PRDM9-dependent H3K4me3 chromatin. *(A)* H3K4me3 ChIP-seq coverage profile showing nucleosome positions and central NDR for *Hlx1* activated by PRDM9^{Cst}. The position of assayed SNPs are shown as circles and the PRDM9^{Cst} binding site as a black bar. *(B)* Position of mapped recombinant sperm from progeny of a cross between B6 and CAST mice (n = 94 recombinant sperm, data re-plotted from Parvanov et al. (2009)). *(C)* ChIP-seq signal showing H3K4me3 nucleosome peaks for hotspot *A3* activated by PRDM9^{Dom2}. The black bar indicates the position of the PRDM9^{Dom2} motif identified here. The green bar indicates the interval of meiotic crossing-over reported in a cross between B6 and DBA/2J mice and the highlighted area on the nucleosome position profile shows the co-conversion zone from Cole et al. (2010b).

Supplemental Figure S1

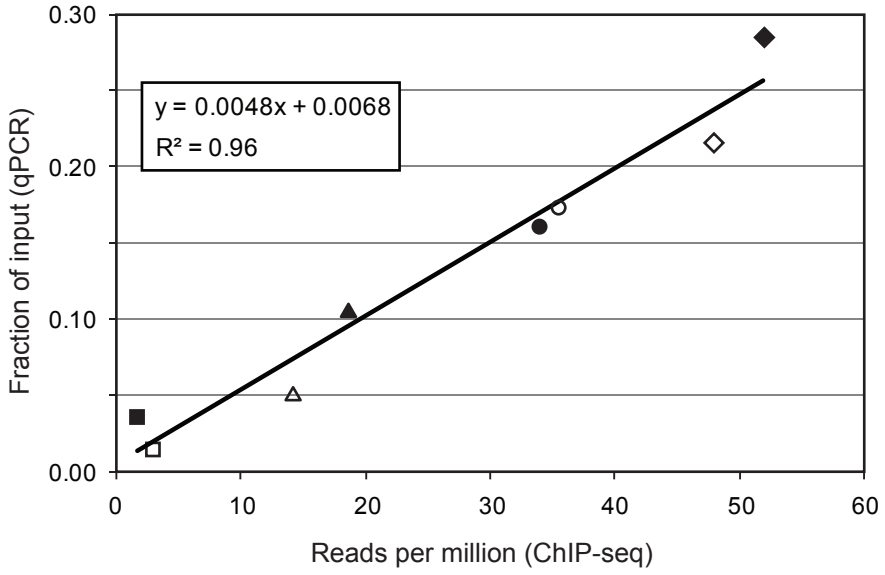

Supplemental Figure S2

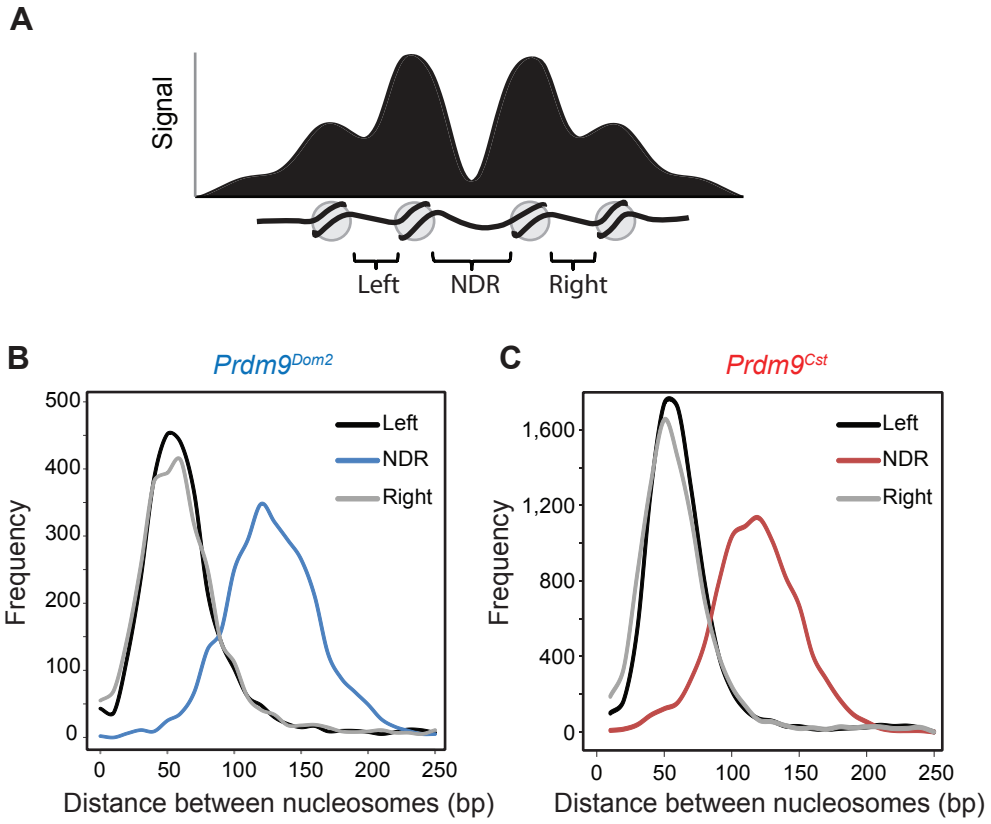

Supplemental Figure S3

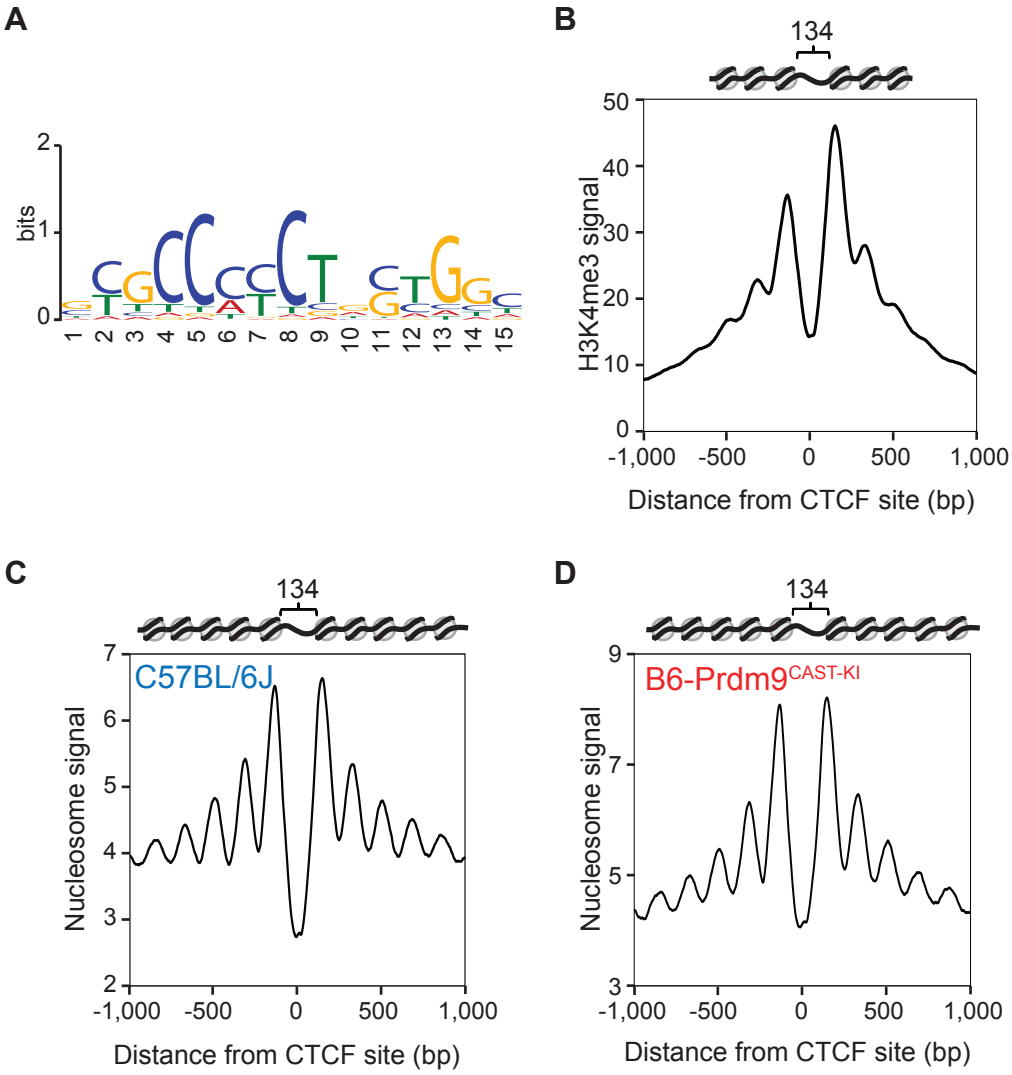

Supplemental Figure S4

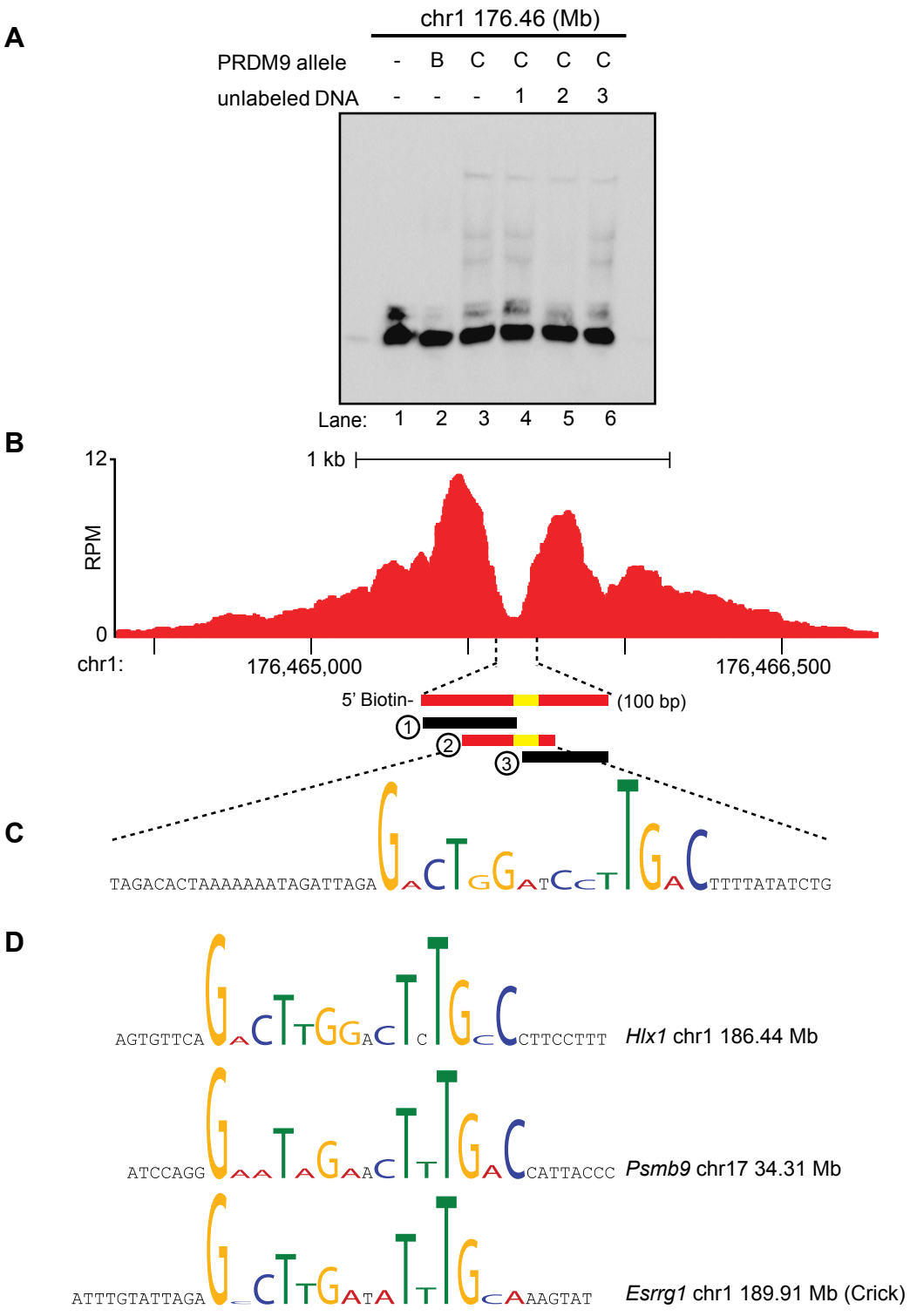

Supplemental Figure S5

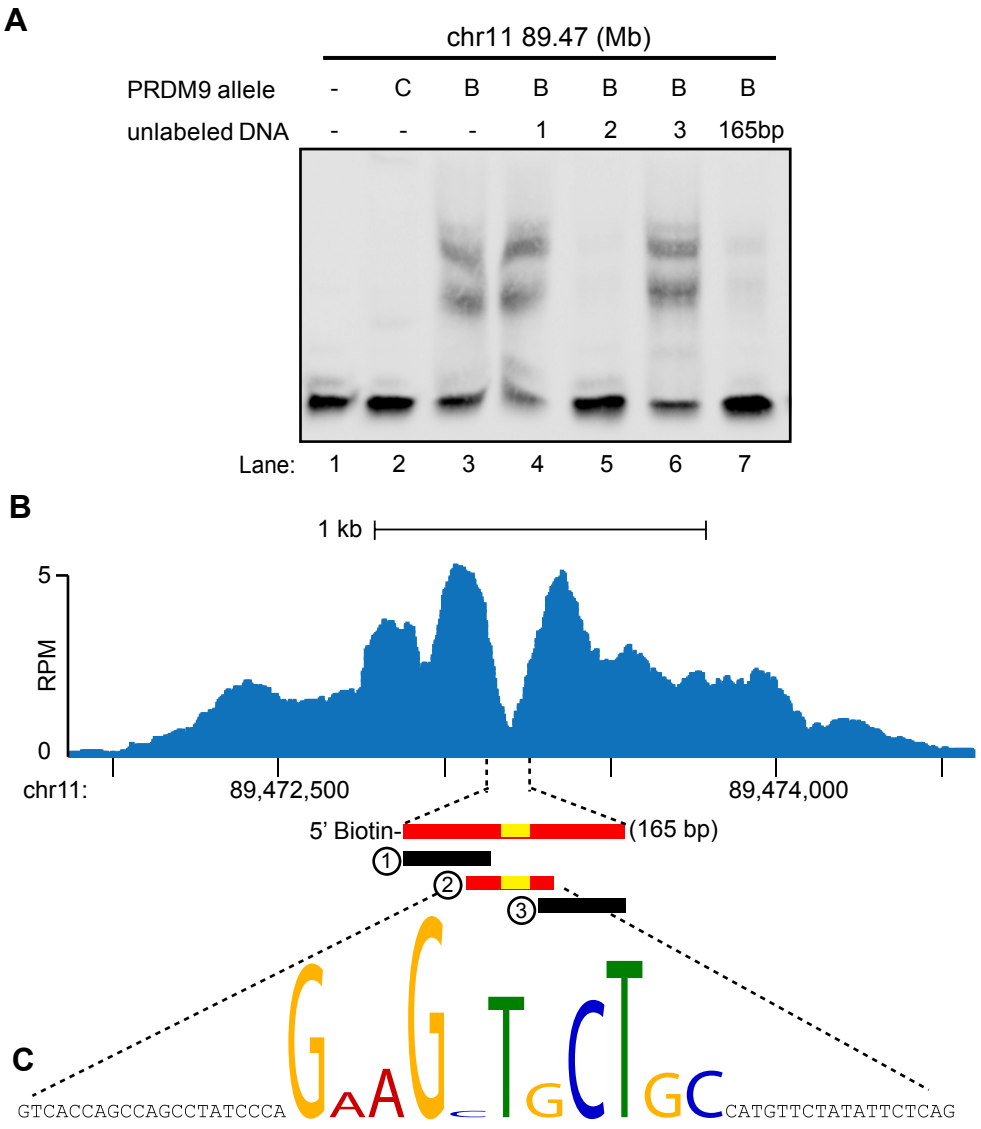

Supplemental Figure S6

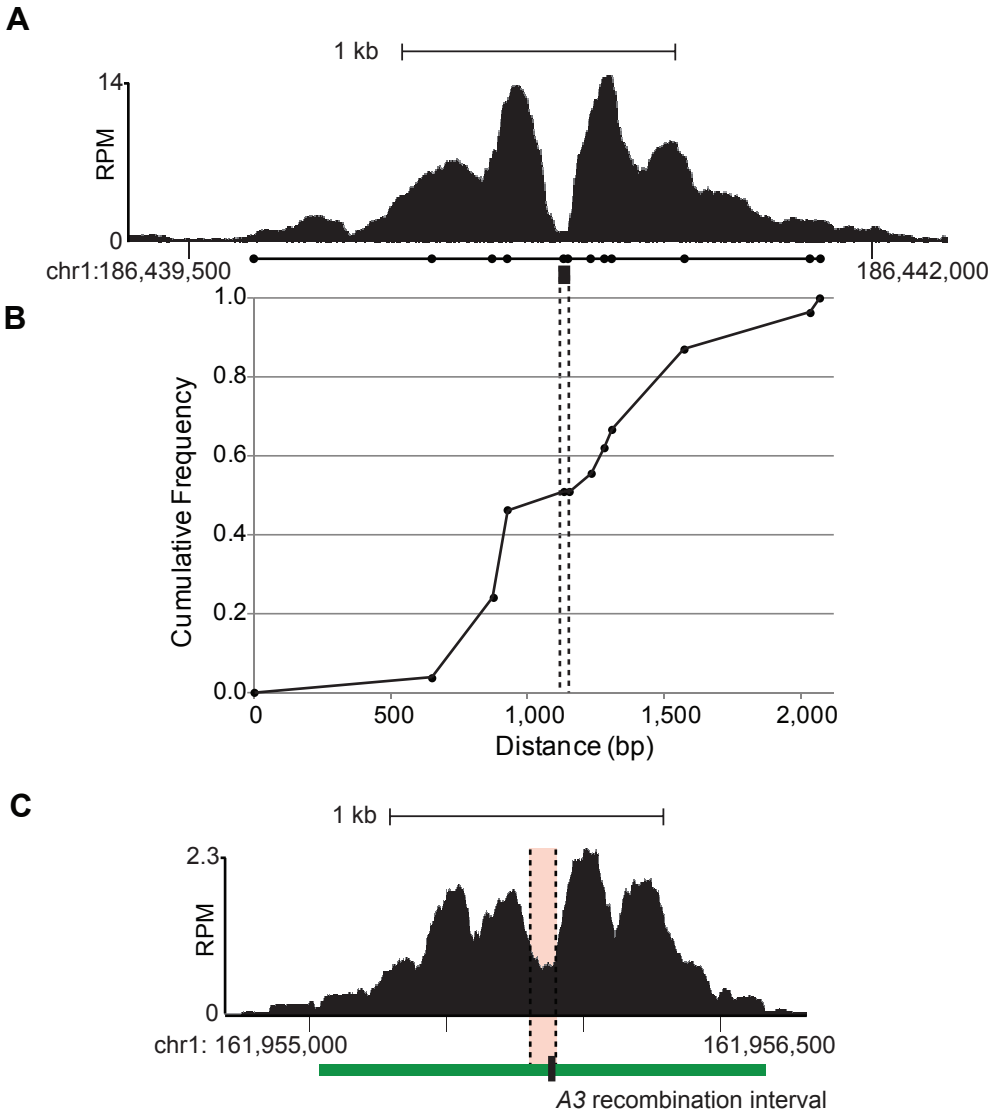

Supplemental Table S1. Primers and synthetic oligonucleotides used in this study

	Name	Sequence
Primers for EMSA	chr19_59.51_F*	ACTCAGTGCTGTTTGTGGG
	chr19_59.51_R	CCTTAGTAGATTGTGGGGAC
	chr19_59.51_1#	TCTCTGGTGGCCCACAAAAGGCACAGGTCTAAAGATGGGACACCAGAAGG
	chr19_59.51_2#	AGGTCTAAAGATGGGACACCAGAAGGTACTGTCCTCCTAAGATACTTATT
	chr19_59.51_3#	TACTGTCCTCCTAAGATACTTATTCTCCACATACTGGTTCATAAGTTGGA
	chr1_171.37_F*	CTGCTACAGATGGAATGTTGC
	chr1_171.37_R	GCTTAGAAGGCAGGTTGACG
	chr1_171.37_Left#	GAATCATATATTGAATTCCTAAACCCAATGTGATAATATTAGAAGGAGGAGGCTTTGAGCCTCAGAAGGAGAGA
	chr1_171.37_Right#	AGGAGGAGGCTTTGAGCCTCAGAAGGAGAGATGAGGCAAGGTCTAATCTCAAGTCAATCGAACTGCTCGAGAGCC
	chr1_171.37_1#	AGGAGGAGGCTTTGAGCCTCAGAAGGAGAGATGAGGCAAG
	chr1_171.37_2#	AGAAGGAGAGATGAGGCAAGGTCTAATCTCAAGTCAATAG
	chr1_171.37_3#	GCAAGGTCTAATCTCAAGTCAATAGAACTGCTCGAGAGCC
	chr11_89.47_seqF	CAAAATAGTGACACAGCTGCG
	chr11_89.47_seqR	CATCAAAGTAGACGCATGCC
	chr11_89.47_F*	CTCTGAAACCTGAAACCTCC
	chr11_89.47_R	CCTCAGTATCCCTGCACTTC
	chr11_89.47_1#	CTCTGAAACCTGAAACCTCCTCAAGAGAGCTGAGCCCAGTCACCAGCCAG
	chr11_89.47_2#	GTCACCAGCCAGCCTATCCCAGAAGCTGCTGCCATGTTCTATATTCTCAG
	chr11_89.47_3#	CTATATTCTCAGGGCTGCCCTGTCACGGGGGAAGTGCAGGGATACTGAGG
	chr1_176.46_F*	CTGCTCACCAGAAAAGTACT
	chr1_176.46_R	GTCACTGTTTGACTCTAAAG
	chr1_176.46_1#	CTGCTCACCAGAAAAGTACTCTAGGTAGACACTAAAAAAATAGATTAGAG
	chr1_176.46_2#	TAGACACTAAAAAAATAGATTAGAGACTGGATCCTTGACTTTTATATCTG
	chr1_176.46_3#	ACTGGATCCTTGACTTTTATATCTGTCTGTCTTTAGAGTCAAACAGTCAA
	chr1_116.85_F*	TAACCCAAGGGAAAGCAGC
	chr1_116.85_R	CTATTAGGTTGTTTAATAC
Primers for qPCR (peak-to-valley ratio)	chr1_88.114_peakF1	CCCACAGTTTCCTTCCGTCTT
	chr1_88.114_peakR1	CCTCTGTATTTCCTAGAACATG
	chr1_88.114_valleyF1	CCTGAGCCGGAAGTTACTAC
	chr1_88.114_valleyR1	AACACAGGCAGGAGCTTGAG
	Hlx1_PeakF	GGTCGGTGTGAGTATTAGACG
	Hlx1_PeakR	GGCTACTATACCTTATGCTCTG
	Hlx1_valleyF	CTGATGTGGGAGGAGATGGT
	Hlx1_valleyR	TGAGAGGCAGAACCTTCCAT
	Pbx1_peakF	ATACAGCTGGCTTGCTTGGT
	Pbx1_peakR	CCCCCTTCCCCATAATACTG
	Pbx1_valleyF	TCACCTATTCAAGGAAGGGACT
	Pbx1_valleyR	CGGTGGTGTAAACACTCCAT
Primers for qPCR (Supplemental Figure S1)	chr2_14.79_F	TGTTTGAGAAGGTAGCAGGTGA
	chr2_14.79_R	CTGTAATCTTGCTGCCGTGA
	chr2_7.55_F	ACTTGACTGGGTTTGGCATC
	chr2_7.55_R	CCACAAGGCTAGGTGGGATA
	chr1_54.93_F	ACCCCAGCTTCCTTTTATCC
	chr1_54.93_R	GCAACGTGCACAGAGAAAAA
	chr1_170.45_F	ATACAGCTGGCTTGCTTGGT
	chr1_170.45_R	CCCCCTTCCCCATAATACTG

* - Primers were ordered with 5´ Biotin

- Reverse compliment was also ordered to anneal for generating dsDNA

All primer coordinates are to the nearest Mb (NCBI Build 37)